



Contents lists available at ScienceDirect

Fuel

journal homepage: www.elsevier.com/locate/fuel



Effects of CO₂ on biomass fast pyrolysis: Reaction rate, gas yields and char reactive properties

C. Guizani*, J.E. Sanz¹, S. Salvador

RAPSODEE, Mines Albi, Route de Teillet, 81013 ALBI CT Cedex 09, France

HIGHLIGHTS

- The CO₂ impacts the biomass pyrolysis process.
- Introducing CO₂ results on a higher CO yield and lower char yield.
- Char reactivity, chemical and textural properties are different in a CO₂-containing atmosphere.
- TPO analysis reveals different oxidation profile for CO₂-chars.

ARTICLE INFO

Article history:

Received 29 May 2013
Received in revised form 22 July 2013
Accepted 25 July 2013
Available online xxx

Keywords:

Biomass pyrolysis
CO₂
Char properties

ABSTRACT

The effect of CO₂ introduction in a biomass fast pyrolysis process at 850 °C was investigated. It was found that CO₂ impacts the final gas yield and composition, and the char yield and properties. Introducing CO₂ in the pyrolysis medium alongside nitrogen enhanced CO production as a result of homogeneous and heterogeneous reactions of CO₂ with gases, tars and char. The char yield was lower compared to a reference char yield in pure nitrogen. The char obtained in a CO₂-containing atmosphere has its surface area increased nearly sixfold and has a chemical composition different from that of chars obtained in N₂ atmosphere. However, the reactivity of the two chars towards H₂O, CO₂ and O₂ was almost the same. Temperature-programmed oxidation experiments on both chars – those obtained in pure nitrogen and those obtained in a CO₂-containing atmosphere – revealed quite different oxidation profiles and peak temperatures. Taken together, these results tend to confirm that CO₂ is impacting the biomass fast pyrolysis process. In the light of these results and of the literature findings, we propose a mechanism illustrating the role of CO₂ during fast pyrolysis of biomass.

© 2013 Published by Elsevier Ltd.

1. Introduction

Biomass pyrolysis is a thermal decomposition of the biomass into gas, liquid, and solid [1]. The yields and distribution of the pyrolysis product depend on various parameters such as the physico-chemical characteristics of the biomass (origin, chemical composition, ash and moisture contents, particle size) and the operating conditions (reactor design, temperature, residence time). The production trends of pyrolysis products as a function of temperature and heating rate are reported in Di Blasi's review [2].

For instance, high temperature and small particle size promote gas production and decrease the char yield [3]. Higher residence times in the reactor are also required to maximise the tar thermal cracking to gas. The particle heating rate – which depends on the particle size and shape, as well as on the operating conditions in

the reactor (temperature and gas flow) – is a key parameter which influences the pyrolysis product yields and the char properties [1,4].

Despite the huge amount of study devoted to biomass pyrolysis and dealing with issues related to the aforementioned parameters, noticeably few papers focus on the gas surrounding the solid and its potential effects on the pyrolysis reaction.

For instance, Zhang et al. [5] investigated the effect of the composition of the pyrolysis medium in the biomass fast pyrolysis process in a fluidized bed gasifier at 550 °C. The pyrolysis mediums were N₂, CO₂, CO, CH₄ and H₂. The authors found that the liquid yield, composition and higher heating value depend on the composition of the pyrolysis bath gas. The pyrolysis in a CO₂ atmosphere was seen to produce less char than in the other atmospheres. The CO₂ yield also decreased compared to the yield obtained in an N₂ atmosphere. With regard to the liquid product distribution, the CO₂ atmosphere led to the highest yield of acetic acid compared to the other atmospheres. The acid products yield under N₂ was 9% while it increased to 16% under CO₂. Ketones yield also

* Corresponding author. Tel.: +33 619572786.

E-mail addresses: guizani.c@gmail.com (C. Guizani), javier.escuderosanz@mines-albi.fr (J.E. Sanz), sylvain.salvador@mines-albi.fr (S. Salvador).

¹ Principal corresponding author.

increased slightly from 15% to 17% while the phenol yield decreased from 33% to 26%. The authors explained these observations by alluding to two possible mechanisms: either the CO₂ reacted with the active volatiles or with the biomass char. The former assumption seems to be more plausible in view of the pyrolysis temperature.

In a recent study, Kwon et al. [6], observed that introducing CO₂ in the macro-algae pyrolysis process resulted in a breakdown of a significant amount of chemical species. The gas yield was enhanced while the oil yield decreased. The same authors performed another study of the pyrolysis of styrene butadiene rubber [7] and found that the CO₂ enhances C4 hydrocarbon cracking in addition to impeding the gas phase addition reaction by which benzene derivatives are formed. Tyre pyrolysis experiments at 650 °C in free and in CO₂-containing atmospheres showed that the amount of condensable hydrocarbons decreased by 30–50% when introducing CO₂. There was also a modification of the end products.

Other studies focused more on the effect of the pyrolysis atmosphere on the char properties. Hanaoka et al. [8] found that preparing chars in a N₂/CO₂/O₂-containing atmosphere leads to a more developed surface area and a higher reactivity towards pure CO₂, especially in a 18% N₂/41% CO₂/41% O₂ atmosphere. The char yield was similar to that obtained under nitrogen. The authors observed an increase in the BET surface area from 275 m²/g in pure nitrogen to 417 m²/g in a 18% N₂/41% CO₂/41% O₂ atmosphere. The char reactivity towards CO₂ also increased by a factor of 1.7 to 2.5 for chars prepared in a CO₂-containing atmosphere.

Jamil et al. [9] performed coal pyrolysis experiments in a wire-mesh reactor respectively under He and CO₂ with slow and high heating rates. The authors found that the nascent char obtained after a fast heating is very reactive to CO₂. The authors proposed that the char gasification with CO₂ occurs simultaneously with the thermal cracking during fast heating. The CO₂ would mainly react with radicals generated at the char surface, which systematically induces an extra mass loss compared to the inert atmosphere.

In a quite recent study, Gao et al. [10] studied the influence of CO₂ in the lignite pyrolysis process. The authors found that CO₂ impacts the lignite pyrolysis process on different levels. They concluded that the introduced CO₂ promotes the occurrence of coal pyrolysis by enhancing the cracking of the benzene ring and the fracturing of hydroxyl, methyl and methylene groups. Further gasification by CO₂ caused the char to have a higher specific surface area and enhanced the gas yield.

Borrego et al. [11] performed pyrolysis experiments on pulverised wood (particle size of 36–75 μm) in a drop tube furnace at 950 °C under N₂ and CO₂. They performed textural characterisation of the residual chars and found similar specific areas: 277 and 331 m²/g under N₂ and CO₂. The char reactivity towards air at 550 °C in a TG device was also the same. The residence time was estimated at 0.3 s.

Other studies have focused more on coal pyrolysis but it is still interesting to analyse their results as a means of comparison with biomass pyrolysis. For instance, Gil et al. [12] performed pyrolysis experiments on pulverised coal chars in a drop tube furnace under N₂ and CO₂ atmospheres at 1000 °C. The authors observed an enhanced volatile yield in the CO₂ atmosphere in comparison with the N₂ atmosphere.

Other studies highlighted the role of CO₂ in oxy-fuel conditions. Rathnam et al. [13] studied the reactivity of pulverised coals in air (N₂/O₂) and oxy-fuel conditions (CO₂/O₂). Experiments were performed in an entrained flow reactor at 1400 °C and the residence time was estimated to be 0.62 s. The authors observed that replacing 79% N₂ by 79% CO₂ alongside O₂ results in a higher volatile yield. The char specific area and reactivity also increased with the introduction of CO₂. The authors imputed these results to the

char-CO₂ reaction occurring simultaneously with the pyrolysis and the combustion reactions.

Thus, according to the literature, the surrounding gas impacts the pyrolysis reaction and product yields. However, very little information about the phenomena involved is available in the literature. The aim of the present study is to assess the effect of the presence of CO₂ in the surrounding gas on the pyrolysis reaction and to deepen understanding of its potential impacts. The present study concerns biomass fast pyrolysis at a high temperature of 850 °C. These experimental conditions come close to those encountered in fluidized bed gasifiers. The potential effects of CO₂ are assessed through the pyrolysis reaction rate, the pyrolysis product yields and composition and the char properties.

2. Materials and methods

2.1. Parent wood sample

The biomass samples were beech wood-chips provided by the French company SPPS. Raw samples were initially sieved. Biomass particles with a size in the range of 4–5 mm and a thickness of about 1 mm were selected to perform the pyrolysis experiments. Proximate and ultimate analysis of the biomass samples are presented in Table 1. The results are given on a dry basis. The moisture content of the wood-chips was 10% ± 1%.

2.2. Experimental devices and procedures for wood-chips pyrolysis

2.2.1. The macro-thermogravimetry experimental device and procedure

The thermal degradation of the wood-chips in a macro-thermogravimetry device (M-TG) was used to determine the pyrolysis rate and final char yield. Experiments were performed under two atmospheres: N₂ and 20% CO₂ in N₂ at 850 °C.

2.2.1.1. M-TG apparatus. The new M-TG device is described in detail in our previous work on char gasification in mixed atmospheres of CO₂ and H₂O [14]. In general terms, the experimental apparatus consists of a 2-m long, 75-mm i.d. alumina reactor that is electrically heated, and a weighing system comprising an electronic scale having an accuracy of ±0.1 mg, a metallic stand placed over the scale on which three hollow ceramic tubes are fixed, each having a length of 1 m and a 2.4 mm external diameter. These ceramic tubes hold up a platinum basket in which the biomass particles are placed. The gas flow rates are controlled by means of mass flow-meters/controllers. The gas flow inside the reactor is laminar and flowing at an average velocity of 0.20 m/s. This device allows fast heating of the biomass particles as they are introduced in the hot furnace within less than 15 s.

2.2.1.2. Experimental procedure. A load of 20 to 25 wood-chips with a total weight of about 0.5 g was placed in the platinum basket and uniformly spaced to avoid thermal and chemical interactions. The biomass particles were submitted to a thermal shock as if they had been placed in a fluidized bed gasifier. For this purpose, a new rapid sample introduction procedure – involving a blank test –

Table 1
Proximate and ultimate analysis of the beech wood-chips (% dry basis).

Proximate analysis			Ultimate analysis			
VM	Ash	FC	C	H	O	N
88.1	0.4	11.5	46.1	5.5	47.9	0.1

had to be developed in order to run short duration experiments. During the heating of the platinum basket and the ceramic tubes, the flowing gas dynamic pressure (force exerted on the basket) in addition to the drag forces along the ceramic tubes caused the displayed mass value to change. Once a thermal equilibrium was reached inside the reactor, and the gas flow around the basket and the ceramic tubes had stabilized, the displayed mass remained constant. Blank tests (without wood-chips in the basket) were performed to correct the mass decay. The reproducibility of the blank tests was verified and an experimental protocol was established so that the pyrolysis tests were always performed in the same way. For data processing, we subtracted the blank test mass record from that of the pyrolysis experiment. Fig. 1 shows reproducibility pyrolysis test results with 20% CO₂ in N₂ after correcting the mass record. The mass loss is recorded via the electronic scale every 0.1 s.

Pyrolysis experiment results were very reliable after 13.5 s; before this time, results remained acceptable except at 2–3 s when lifting the device and at 11–12 s when stopping the motion of the device. One can note a time delay of approximately 8 s before the particle mass loss began, which was attributed to the heating of the metal basket.

2.2.2. The horizontal tubular reactor experimental device and procedure

To determine the effect on the gas yield and composition of introducing the CO₂, pyrolysis experiments were performed on the wood-chips in a Horizontal Tubular Reactor (HTR) at 850 °C under three different atmospheres: N₂, 20% CO₂ in N₂ and 40% CO₂ in N₂.

2.2.2.1. HTR apparatus. The Horizontal Tubular Reactor (HTR) consists of a double-walled quartz pipe. The length and inside diameters are respectively 850 mm and 55 mm for the inner tube, and 1290 mm and 70 mm for the outer tube. Nitrogen and carbon dioxide flow rates are controlled by means of mass flow-meters/controllers. The major part of the incoming gas flow (75%) is introduced on right hand-side of the reactor and passes through the annular space to be heated before reaching the biomass samples. The rest of the gas flow is injected on the left hand-side to cool the injection spoon when pooled out from the hot zone and to prevent a backward flow of the pyrolysis gases. The pyrolysis experimental device is presented in Fig. 2.

2.2.2.2. Experimental procedure. A load of 20–25 wood-chips with a total weight of about 0.5 g was placed in a basket made with a stainless-steel grid of 0.5 mm thickness and attached to the end of a mobile stick made of Pyrex. The wood-chips were spaced widely enough to avoid chemical and thermal interactions. The mobile stick bearing the basket containing the biomass samples was kept in the non-heated zone until the stabilization of the

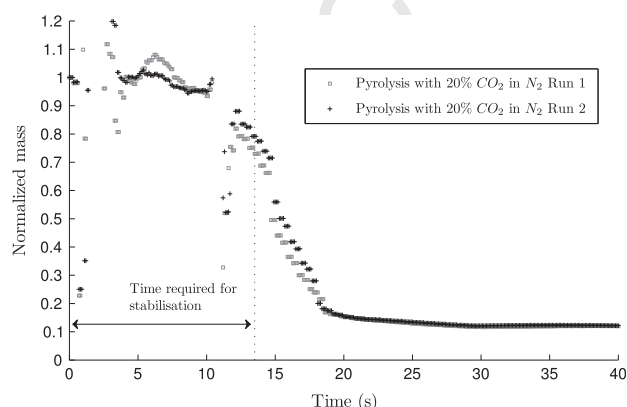


Fig. 1. Repeatability tests of high-temperature flash pyrolysis experiments.

reactor atmosphere. The flow rate of the pyrolysis gas medium (pure nitrogen or mixtures of carbon dioxide and nitrogen) was set to 2 l/min (STP). Part of the gas flow was initially deviated to a SERVOMEX paramagnetic analyser to quantify the oxygen. Once the O₂ concentration reached zero, the pyrolysis experiment could start. At $t = 0$, the reactor outlet was connected to a Tedlar gas sampling bag. Then, the mobile stick was introduced in the hot reactor until the grid basket reached the entry of the isothermal zone, which had a length of 40 cm and a temperature of 850 ± 10 °C. The gas collection time was set to 3 min according to preliminary pyrolysis tests showing that the pyrolysis reaction lasts less than 1 min. When CO₂ was introduced alongside nitrogen, the stainless-steel basket was pulled out in the cooled zone after 1 min to avoid char gasification by CO₂. CO₂, CO, H₂, CH₄, C₂H₄ and C₂H₂, which are the major permanent gases emitted during pyrolysis, were subsequently analysed with a micro-chromatograph analyser (Agilent 3000 μ GC). As the pyrolysis emitted a considerable amount of water (0.10–0.17 g/g wood (db)), calculations and precautions were made to ensure that the water partial pressure in the bag was below its saturation pressure to avoid water condensation inside the bag, which could distort the measurements. We also filled the bag periodically with air to force any eventually condensed water to evaporate.

2.2.2.3. Pyrolysis product yields. N₂ was used as a gas tracer. As the quantity collected in the bag was known, and its molar fraction was given by the μ GC, it was possible to determine the total moles of gas in the bag:

$$n_{tot} = \frac{n_{N_2}}{x_{N_2}} = \frac{Q_{N_2(STP)} \times \rho_{N_2(STP)} \times t_{sampling}}{M_{N_2} \times x_{N_2}} \quad (1)$$

and to calculate the molar quantity of the aforementioned gaseous species:

$$n_i = x_i \times n_{tot} \quad (2)$$

With: n_{tot} : total gas moles [moles], n_{N_2} : nitrogen moles [moles], x_{N_2} : nitrogen molar fraction, $Q_{N_2(STP)}$: nitrogen flow rate [l/min], $\rho_{N_2(STP)}$ nitrogen density [kg/m³] and $t_{sampling}$: sampling duration [min].

The results are given hereafter as mass yields on a dry ash-free basis (kg gas/ kg wood (dafb)). The total gas yield represents the mass of permanent gases emitted during the pyrolysis (daf):

$$Y_{gas} (\%) = \frac{m_{gas}}{m_{wood(dafb)}} \times 100 = \frac{\sum m_i}{m_{wood(dafb)}} \times 100 \quad (3)$$

The energy content of the gas is assessed through the variable CGE (cold gas efficiency). This variable represents the ratio between the energy content of the permanent gas (HHV_{gas}) and the energy content of the initial biomass feedstock ($HHV_{wood(dafb)}$) without taking into account the heat input in the reactor:

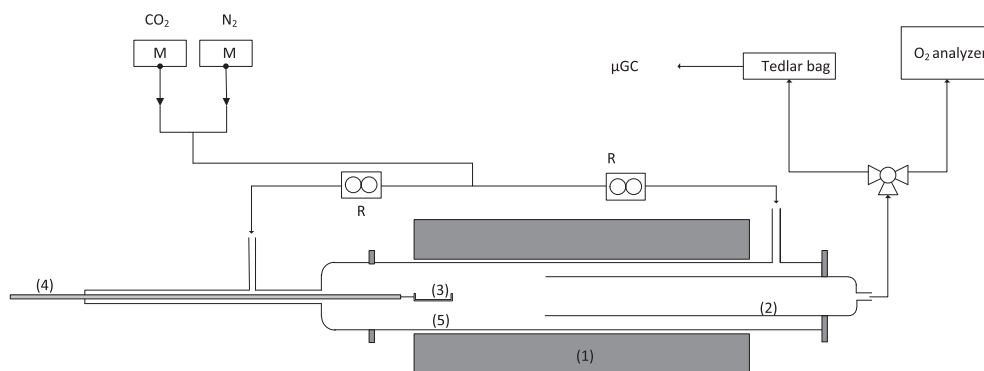
$$CGE = \frac{HHV_{gas}}{HHV_{wood(dafb)}} \quad (4)$$

At the end of the experiment the residual chars were weighed and stored in a sealed recipient for further characterisation. The char yield is expressed as the ratio of the residual char to the initial mass of wood (db)

$$Y_{Char} (\%) = \frac{m_{Char}}{m_{wood_{db}}} \times 100 \quad (5)$$

2.2.3. Similarity of the experimental conditions in both reactors

A fact worth noting is that we characterised the M-TG and HTR reactors in terms of flow properties and heat transfer coefficients at



1-furnace (heating element); 2-inner tube; 3-grid sample holder; 4-mobile pyrex stick
5-quartz tubular reactor; M-mass flowmeter/controller; R-rotameter

Fig. 2. Horizontal tubular reactor experimental device.

sample surface. The global heat transfer coefficient at sample surface in the two reactors was determined following a lumped capacitance method [15], and the contributions of both convection and of radiations were estimated. Details about the procedure are given in Appendix A. The gas flow inside the two reactors was laminar. The Reynolds number was estimated to be 13.4 in the M-TG reactor and 3.7 in the HTR reactor. The results for the global heat transfer coefficients in the M-TG and in the horizontal tubular reactor are given in Table 2.

Given the similarities in the gas flow properties, in the global heat transfer coefficients and heat transfer mode (the same magnitude and radiative for more than 80%), it can be stated that the operating conditions in both reactors are similar and that it is legitimate to establish comparisons between experiments performed in the two experimental devices.

Based on the above results, we also estimated the initial heating rate of the biomass particle β_0 to be respectively 122 and 101 [K/s] in the M-TG and in the HTR reactor [16]. Details are given in Appendix B.

2.3. Characterisation of the remaining char

To determine if pyrolysing wood under a CO₂-containing atmosphere impacts on the char properties, we performed a set of characterisation tests and reactivity measurements with CO₂, H₂O and O₂ of chars obtained respectively after pyrolysis in pure nitrogen and pyrolysis in 20% CO₂ in N₂.

2.3.1. Chemical composition

The remaining char chemical composition was determined by ultimate analysis in terms of C, H, O and N contents. The ash content was determined by combustion of 100 mg of char in a muffle furnace at 550 °C.

2.3.2. Textural and structural characterisation of the remaining char

Observations of the char structure were made through a Scanning Electron Microscopy (SEM) device. The chars were also characterised for specific surface measurement. The Brunauer–Emmett–Teller (BET) surface area was determined respectively for

Table 2

Flow properties, convective and radiative heat transfer coefficients and particle heating rate in the M-TG and HTR experimental devices.

Reactor	M-TG	HTR
h_{conv} (W/m ² K)	26	20.3
h_{rad} (W/m ² K)	104.7	178.7

chars pyrolysed under N₂ and 20% CO₂ in N₂ in a Micrometrics, Gemini instrument using liquid nitrogen at 77 K. Chars were out-gassed under vacuum for 24 h prior to the gas adsorption experiments in order to eliminate moisture or any condensed volatiles which could prevent the adsorbate from gaining access.

2.3.3. Char reactivity measurement

After the pyrolysis step in the M-TG reactor, we performed gasification tests on the residual chars with steam, carbon dioxide and oxygen. The gasification experiments were made respectively with 20% CO₂ in N₂, 20% H₂O in N₂ and 5% O₂ in N₂. The chars were kept in the furnace and the atmosphere composition was switched to that of the gasification conditions.

The char conversion level is given by:

$$X_{(t)} = \frac{m_0 - m_{(t)}}{m_0 - m_{ash}} \quad (6)$$

where m_0 , m_t and m_{ash} are respectively the initial mass of char, the mass at a time t and the mass of the residual ash.

The char reactivity was calculated over time following the relation:

$$R_{(t)} = \frac{1}{1 - X_{(t)}} \times \frac{dX_{(t)}}{dt} \quad (7)$$

2.3.4. Temperature programmed oxidation

The temperature-programmed oxidation (TPO) technique provides relevant information about the carbonaceous material contained in the chars. Oxidation profiles of the chars in non-isothermal conditions can inform about the type of carbon materials and their peak oxidation temperatures. For instance, it is possible to distinguish between different forms of carbons if the char oxidation profile exhibits more than one peak. Temperature-programmed oxidation (TPO) experiments were performed on the chars obtained in N₂ and in 20% CO₂ in N₂. The char samples were firstly ground gently with a mortar and pillar. A sample mass of 2–4 mg was mixed with 100 mg of silicon carbide (SiC) and introduced in an electrically-heated quartz reactor. First, a temperature-programmed desorption with 50 ml/min of helium was performed from room temperature up to 900 °C with a slope of 15 °C/min in order to clean the char surfaces of any exterior deposit. Then, after cooling and return to baseline, an oxidising gas mixture of 1% oxygen in helium (total flow of 50 ml/min) was introduced in the reactor. The temperature was increased at a rate of 15 °C/min from room temperature to 900 °C. The CO₂ emitted during the char oxidation was monitored by a Mass Spectrometer (Quadrupole Pfeiffer Omnistar).

Q1

C. Guizani et al./Fuel xxx (2013) xxx–xxx

5

385 **3. Results and discussion**

386 **3.1. Pyrolysis rate**

387 High-temperature fast pyrolysis tests show a good repeatability
388 with the established protocol. The data presented hereafter are
389 average values from at least two experiments. The results of pyro-
390 lysis experiments in N₂ and 20% CO₂ in N₂ are shown in Fig. 3. In
391 the figure, a mass loss of 10% at the beginning, perhaps attributable
392 to particle drying, has been indicated. Devolatilisation can be di-
393 vided into two stages: an active phase corresponding to the major
394 mass loss, and a passive phase within which the rate of mass loss
395 decreases abruptly corresponding to lower emissions of gas and
396 tars [17]. It can be seen that the pyrolysis reaction rate is almost
397 the same for pyrolysis under N₂ and for pyrolysis under 20% CO₂
398 in N₂.

399 **3.2. Final char yield**

400 In M-TG pyrolysis experiments, an additional mass decay was
401 observed when the CO₂ was introduced, which resulted in a lower
402 char yield. The char yields after pyrolysis in N₂ and in 20% CO₂ in
403 N₂ at t = 60 s were respectively 13.1 ± 0.3% and 11.32 ± 0.25%.
404 These results indicate that either less char was formed, or that
405 there was a char consumption when introducing CO₂ along with
406 nitrogen.

407 In HTR experiments, a decrease in the char yield from
408 11.7% ± 0.04 down to 10.5% ± 0.38 in a 20% CO₂ containing atmo-
409 sphere was also observed. The char yield remained constant when
410 increasing the CO₂ concentration further to 40%, as shown in Fig. 4.

411 These results confirm those obtained in pyrolysis experiments
412 in the M-TG device, although the decrease in the final mass of
413 the char in pyrolysis experiments with CO₂ was slightly smaller.
414 It is also worth noting that the char mass remained constant even
415 after the CO₂ partial pressure was increased to 40%.

416 The mass of the residual char is known to depend on the tem-
417 perature and on the pyrolysis heating rate [2,4,18]. The final tem-
418 perature was the same in the two experiments. The additional
419 mass loss may be due to a thermal effect or to a chemical effect
420 prompted by the CO₂.

421 As regards thermal effects, the higher specific heat of CO₂ in
422 addition to its radiative properties in comparison to N₂ can modify
423 the heating rate of particles when introduced in the pyrolysis
424 medium. To verify this, we measured the global heat transfer
425 coefficient h_{global} in both atmospheres, keeping the gas velocity
426 constant. We found a slight increase when adding the CO₂, but
427 the order of magnitude was the same: 131 and 148 [W/m² K]
428 respectively. The thermal effect is thought to be negligible.

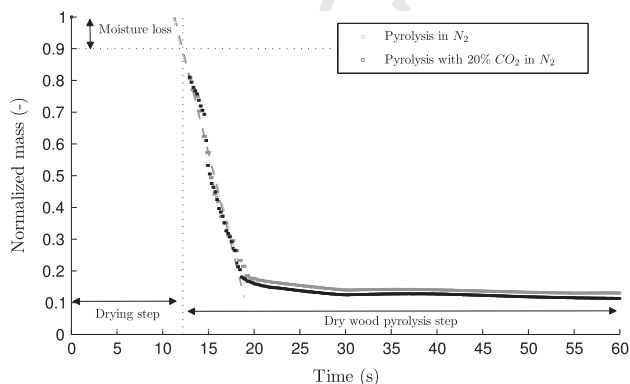


Fig. 3. High temperature flash pyrolysis of beech wood-chips in N₂ and in 20% CO₂ in N₂ (M-TG).

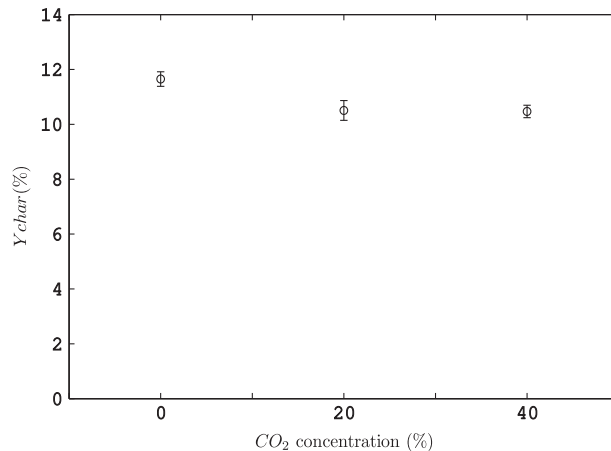


Fig. 4. Char yield as a function of the CO₂ concentration in the pyrolysis medium (HTR).

429 As for the potential chemical effects, there are two possibilities:
430 (i) the CO₂ can inhibit secondary char formation by reacting with
431 tars, and (ii) the CO₂ may react directly with the char according
432 to the Boudouard reaction. At this level, we can not go beyond
433 assumptions with regard to the mechanisms that may be unfold-
434 ing. These assumptions will be discussed later.

435 **3.3. Final gas yields**

436 Fig. 5 shows the pyrolysis gas yields under 100% N₂, 20% CO₂
437 and 40% CO₂ in N₂. Note that the CO yields were divided by 10
438 to fit the figure.

439 We can see that the major change involved the carbon monox-
440 ide. A net increase was observed for CO, whose yield increased
441 from 427 (g/kg wood (daf)) in pure nitrogen to 520 (g/kg wood
442 daf) when introducing 20% CO₂, and further to 561 in a 40% CO₂-
443 containing pyrolysis atmosphere. The CH₄ and C₂ hydrocarbons
444 yield increased slightly in a 40% CO₂ atmosphere compared to a
445 free CO₂ atmosphere. The H₂ yield decreased slightly from 11.8
446 to 11.4 (g/kg wood daf) when increasing the CO₂ concentration
447 from 0 to 40%. In a nitrogen atmosphere, the CO₂ was produced
448 with a yield of 168 (g/kg wood daf). It was not possible to give a
449 reliable result on the CO₂ yield in pyrolysis experiments with
450 CO₂ introduction due to high uncertainties: the amount of pro-
451 duced CO₂ is much smaller than the amount of CO₂ introduced in
452 the atmosphere gas (ratio of 60 approximately) as the introduced

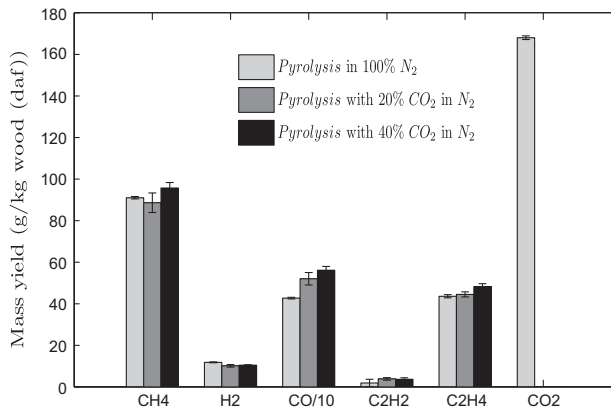


Fig. 5. Pyrolysis gas yields at 850 °C under 100% N₂, 20% CO₂ and 40% CO₂ in N₂ (HTR).

CO₂ to biomass ratio was calculated to be 6.5 and 13 g/g wood (daf) respectively for experiments done with 20% CO₂ and 40% CO₂ in N₂.

The total permanent gas yield (excluding CO₂) increased with the increase in the CO₂ concentration in the pyrolysis medium from 576 (g/kg wood (daf)) in a free CO₂ medium to 667 (g/kg wood (daf)) with 20% CO₂ and further to 719 (g/kg wood (daf)) with 40% CO₂ in the pyrolysis medium. The energy content represented by the variable CGE increased accordingly by 13% from 0.66 (0% CO₂) to 0.75 (40% CO₂). However the H₂/CO ratio decreased with the increase in the CO₂ concentration in the pyrolysis gas medium.

3.3.1. Interpretation and discussion of results

As mentioned in the introduction section, several studies have dealt with the effects of CO₂ in biomass and coal pyrolysis. For instance, Kwon et al. [6] found that introducing CO₂ alongside nitrogen in the pyrolysis process at 550 °C in a tubular reactor decreased the generation of pyrolytic oil and enhanced pyrolytic gas production. The authors propose that hydrocarbons emitted in the pyrolysis process can be broken down in the presence of CO₂, or at least not formed. The authors also carried out steam gasification tests at higher temperatures (600–1000 °C) and noticed that the yield of C2 hydrocarbons also increased and the amount of tar was reduced by 51.2%.

In a more recent study the same authors [7] found that the CO₂ enhances cracking of C4 hydrocarbons in addition to impeding the gas phase addition reaction by which benzene derivatives are formed. The authors also made tyre pyrolysis experiments at 650 °C in a CO₂-free and in a CO₂-containing atmosphere. They found that the amount of condensable hydrocarbons decreased by 30–50% when introducing CO₂ in addition to there being a modification of the end products. The authors proposed that the CO₂ participates in the cracking reactions as well as impeding other reactions by which tars are formed.

In another study, Zhang et al. [5] investigated the effect of the pyrolysis medium composition on the biomass fast pyrolysis process in a fluidized bed gasifier at 550 °C. The pyrolysis in a CO₂ atmosphere was seen to produce less char than in the other atmospheres. The CO₂ yield decreased and the CO yield increased compared to N₂ atmosphere. Moreover, the CO₂ atmosphere led to the highest yield of acetic acid compared to the other atmospheres. Ketones yield also increased in a CO₂ atmosphere while the phenol yield decreased. The authors explained these observation by two possible mechanisms: the CO₂ reacted with the active volatiles or with the biomass char. The former assumption seems to be more plausible in view of the pyrolysis temperature.

Ahmed et al. [19] also evidenced a CO₂ consumption during the pyrolysis of cardboard and paper.

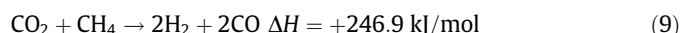
Based on these literature findings, it is clear that CO₂ influences the pyrolysis process by modifying the product yields. One of the major findings is that the CO₂ hinders condensable hydrocarbon formation and enhances the CO yield.

Primary tars can undergo polymerisation reactions and form secondary char as proposed by Gilbert et al. [20] and Zhang et al. [21]. According to the literature findings, a plausible explanation for the char mass decay may be that the CO₂ prevents tar polymerisation reactions and secondary char formation. The decrease in the final mass of char and the increase in the gas yield may be due to the enhanced tar cracking by CO₂ according to:

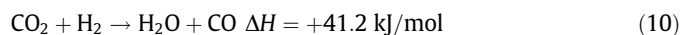


The CO₂ may also participate in homogeneous gas reforming reactions, as reported by Sutton et al. for methane and propane reforming [22].

Methane dry reforming reaction (MDR) by CO₂ is promoted at high temperatures (thermodynamically possible above 640 °C) and leads to an enhanced CO production according to:



The CO₂ can also react with hydrogen molecules according to the reverse water gas shift reaction (rWGS), which is the dominant reaction at high temperature (above 700 °C):



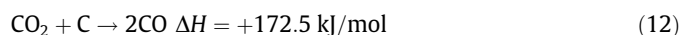
The observations of improved gas yields at low temperature found in the literature are probably related to homogeneous reactions and tar cracking by CO₂. A straightforward thermodynamic approach based on the Gibbs available energy variation shows that at temperatures below 650 °C, the Boudouard reaction does not promote CO formation (1) but on the contrary its disproportionation (2) into CO₂ and carbon deposit.



At a high temperature of 850 °C, the char gasification reaction must be taken into account, especially when the pyrolysis is performed at a high heating rate. Jamil et al. [9] performed coal pyrolysis experiments in a wire-mesh reactor respectively under He and CO₂ with heating rates of 1 °C/s and 1000 °C/s from ambient to a prescribed peak temperature. They found that, in fast pyrolysis experiments, the char yield in CO₂ is slightly but systematically lower than that in He over the range of the holding time. The difference in the char yield was in the range 1–2 wt.-%-daf at a peak temperature of 700 °C, but was outside the range of experimental error. Fast heating rate pyrolysis up to 800 °C showed a difference in the char yields in the range of 2–3 wt.-%-daf from the very beginning of the holding time period at this peak temperature. These results confirm the observations made in the present study concerning the lower char yield in a CO₂-containing pyrolysis atmosphere. The authors went further in investigating this observation and concluded that fast pyrolysis (high heating rate) improves the thermal cracking of the char and provides high concentrations of radical species at the char surface, compared to a slow pyrolysis. These radicals constitute the active sites and are very reactive towards CO₂ molecules. The authors proposed that the rate of the gasification reaction is closely related to the rate of the thermal cracking that generates the radicals. The reactivity of the nascent char towards CO₂ during fast heating from 600 to 900 °C was two or more orders of magnitude higher than reactivity data found in the literature for similar coal chars.

These observations, made by Jamil et al., can explain the additional mass decay observed in our experiments. The nascent char obtained after the fast pyrolysis may contain a high concentration of radicals at its surface, which reacted with the surrounding CO₂ and led to the char consumption.

Di Blasi reported in her review a panoply of kinetic rate constants for the CO₂-char gasification reaction of numerous biomasses [2]. A characteristic time approach shows that the rate of the Boudouard reaction is low at 850 °C. However, the mechanisms of the char gasification seems to be different for a nascent char prepared at a high heating rate [9]. The Boudouard reaction is therefore a potential cause behind CO yield increase and char mass decay:



Taking the results obtained in the present study together with the literature analysis, the improved CO yield and the final char mass decay can be the result of three combined effects of improved tar cracking by CO₂: the gas phase reactions of methane reforming

Q1

7

585 and reverse water gas shift, and char gasification. The next sections
586 will shed more light on the pyrolysis process unfolding in a CO₂-
587 containing atmosphere.

588 3.3.2. Effect of CO₂ co-feeding on the char properties

589 3.3.2.1. Structural and textural properties.

590 • SEM analysis

591 Fig. 6 shows SEM images of chars pyrolysed at 850 °C under N₂ and
592 20% CO₂ in N₂. Both chars show a similar amorphous, heteroge-
593 neous and disordered structure. No clear difference was
594 observed between the two char structures, both of which kept
595 the fibrous aspect of the raw wood with extensive cracks and
596 breakages, probably due to the violent release of volatiles dur-
597 ing the pyrolysis stage.

598 • Char specific area measurement

599 Fig. 7 shows the N₂ adsorption isotherms of two chars. The re-
600 ported data are the average of two repeatability experiments.

601 The adsorbed volume of N₂ per unit mass of porous carbon
602 (char) is more than 6 times greater for chars prepared with 20%
603 CO₂ in the heating medium than those obtained with a pure N₂
604 heating medium. The respective BET specific surfaces are
605 68.9 ± 14.33 m²/g and 408.3 ± 3.1 m²/g. Former studies showed
606 the same order of magnitude for the specific area of chars prepared
607 with a high heating rate under nitrogen: $S_{BET} < 70 \text{ m}^2/\text{g}$ [4]. The
608 specific area greatly expanded in the presence of CO₂. In a study
609 on biomass char pyrolysis in a drop tube furnace respectively under
610 N₂ and CO₂ [11], Borrego et al. performed textural characterisa-
611 tion on wood-chip chars and found similar specific areas: 277 and
612 331 m²/g respectively under N₂ and CO₂. The char reactivity to-
613 wards air at 550 °C in a TG device was also the same. The operating
614 conditions were not the same (particle size of 36–75 µm, residence
615 time of 0.3 s and reactor temperature of 550 °C), which makes the
616 comparison rather difficult. However, in another study, Klinghoffer
617 et al. prepared biomass chars in a fluidized bed reactor with a heat-
618 ing rate of 20°/min under steam and CO₂. They found that the chars
619 were active with respect to hydrocarbon cracking. The chars exhib-
620 ited similar surface areas in the range of 400–700 m²/g depending
621 on the operating conditions. However the char yield in a CO₂ me-
622 dium is highly micro-porous. The authors imputed this micro-poro-
623 sity to the CO₂, which is in accordance with our findings [23].

624 The physical activation of chars by CO₂ for activated carbon
625 preparation has been extensively studied, and it is well established
626 that the CO₂ develops the microporosity inside the char [24,25].
627 However, such char activation procedures for microporosity
628 development are quite different, as they usually involve several
629 steps of pyrolysis, carbonisation at high temperature with holding
630 times exceeding sometimes 1 h, and finally char gasification by
631 CO₂ for extensive microporosity development. In their review on
632

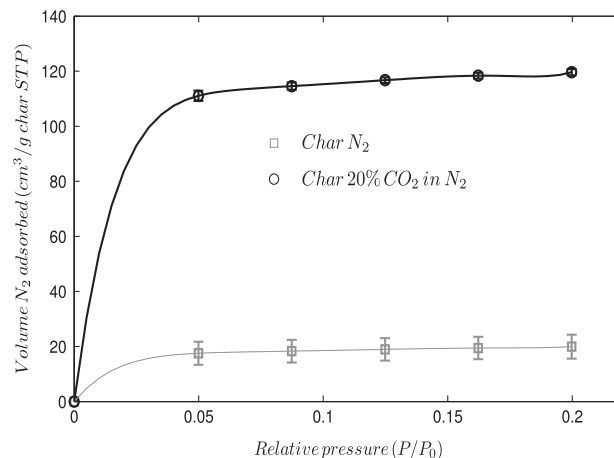


Fig. 7. N₂ adsorption isotherms of beech wood chars pyrolysed respectively under pure nitrogen and 20% CO₂ balanced with nitrogen (HTR).

633 carbon molecular sieve preparation from lignocellulosic biomass,
634 Mohammed et al. reported on the experimental conditions and
635 procedures for preparation of highly porous materials by CO₂ acti-
636 vation. The experimental procedures are usually of long duration,
637 involving a chemical activation step, a pyrolysis/carbonisation step
638 that may lasts from 1 to 8 h, and a CO₂ or steam activation step
639 whose duration is in the range of 15 to 1080 min. The char burn-
640 off is also high in the range of 34 to 80% [26]. These procedures
641 are, in most cases, time- and energy-consuming. In the present
642 study, the char specific area increased sixfold within a very short
643 duration and using a quite simple one-step procedure. The high
644 heating rate coupled to CO₂ introduction during pyrolysis are pro-
645 cedures worthy of consideration for the effective production of
646 porous carbon material with a good surface area.

647 • Char chemical composition

648 The proximate and ultimate analysis of the two chars are pre-
649 sented in Table 3.

650 The ultimate analysis showed a difference in the chemical
651 composition of the two chars. Indeed, we observe that the hydrogen,
652 oxygen and nitrogen amounts decreased in the 20%CO₂-char. It
653 seems that the functional groups containing oxygen and hydrogen
654 are removed preferentially under CO₂. The hydrogen amount de-
655 creased by 60% and that of oxygen by 18%.

656 The H/C and O/C ratios of the CO₂-char decreased in comparison
657 with the N₂-char. Adding carbon dioxide into the pyrolysis at-
658 mosphere enhances hydrogen and oxygen loss and carbon enrichment
659 of the residual char. Another fact worth noting is that the ash
660

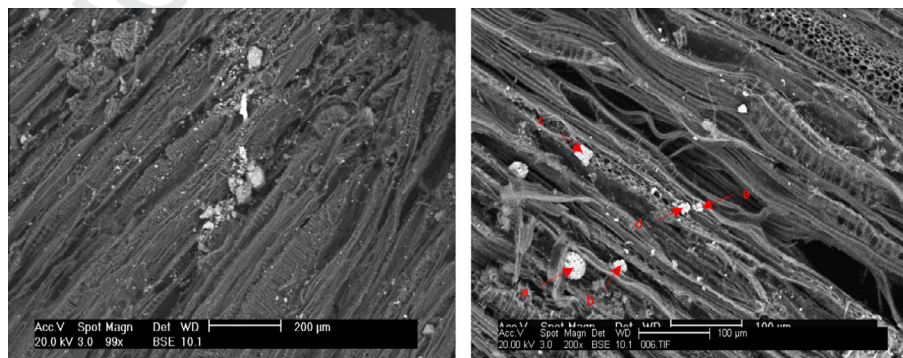


Fig. 6. SEM images of chars obtained at 850 °C respectively under N₂ and 20% CO₂ in N₂ (HTR).

Table 3
Proximate and ultimate analysis of chars obtained under N₂ and 20% CO₂ in N₂ (% dry basis).

	Proximate analysis		Ultimate analysis			
	Ash		C	H	O	N
N ₂ -char	3.00 ± 0.24		87.91 ± 0.81	1.97 ± 0.56	6.16 ± 0.04	0.96 ± 0.28
CO ₂ -char	3.79 ± 0.15		89.82 ± 0.51	0.78 ± 0.17	5.05 ± 0.23	0.63 ± 0.09

amount increased for the 20%CO₂-char, which is synonymous of char conversion and confirms the char yield decrease when CO₂ is added in the pyrolysis atmosphere.

3.3.2.2. Char reactivity measurements. The reactivity tests on the two chars with alternatively 20% of steam in N₂, 20% CO₂ in N₂ and 5% O₂ in N₂ were performed after the pyrolysis step by switching the reactor atmosphere to the desired composition (CO₂, H₂O and O₂). The purpose here was to characterise the influence of the pyrolysis atmosphere composition on the char reactivity. Reactivity profiles along the char conversion are shown in Fig. 8. These reactivity results are the average of three repeatability tests. The mean reactivities ($X = 0.2-0.9$), as well as the standard deviations (error bars), are presented in Fig. 9.

In steam gasification experiments (Fig. 8.a), we observed that the char reactivity profiles remained the same regardless of the pyrolysis atmosphere composition, and the average reactivities (between $X = 0.2$ and $X = 0.9$) are respectively 0.0081 and 0.0083 (g/g s) for chars obtained in N₂ and in 20% CO₂ in N₂ pyrolysis atmosphere. In the char gasification experiments with CO₂ (Fig. 8.b), we observed an increase in the char reactivity towards CO₂ for the chars prepared in a CO₂-containing pyrolysis atmosphere, especially in the earlier stages of the gasification reaction (up to 40% of conversion). The average reactivities are respectively 0.0028 and 0.0038 (g/g s) for chars obtained in N₂ and in 20% CO₂

in N₂ pyrolysis atmosphere, which represents an increase of 26% in the reactivity (the relative standard deviation is below 5%). This tendency may be explained by the higher surface area of chars obtained in a CO₂-containing pyrolysis atmosphere which influences the Boudouard heterogeneous gasification reaction. The CO₂ diffusion to the carbon active sites can be promoted by this developed surface area, which explains the higher reactivity in the initial stages of the gasification. In fact, total pore volume was estimated to be 0.185 cm³/g for chars prepared with a CO₂-containing atmosphere, while it was only 0.031 cm³/g for chars obtained under N₂. In a more recent study [8], Hanaoka et al. found that preparing chars in an N₂/CO₂/O₂ atmosphere leads to a more developed surface area and a higher reactivity towards pure CO₂, especially in a 18% N₂/41% CO₂/41% O₂ atmosphere. The char yield was similar to that obtained under nitrogen but there was an increase in the BET surface area from 275 m²/g in pure nitrogen to 417 m²/g and an increase in the char reactivity by a factor of 1.7 to 2.5 depending on the gasification temperature.

Despite the micro-porosity that developed in chars prepared in a CO₂-containing atmosphere, their reactivity towards steam was the same as that of chars prepared in N₂. Micro-porosity does not seem to influence the char-steam gasification reaction. This can be explained by the difference in char porosity development with both gases [24]. In fact, it has been demonstrated that submitting a char to activation with steam or CO₂ does not lead to the same porosity development. The CO₂ promotes the development of narrow microporosity up to about 20% burn-off, followed by a widening up to about 40% burn-off. On the other hand, steam widens the microporosity from the earlier stages of the gasification [25]. This observation can explain why a developed microporosity enhances the reactivity of the char towards CO₂ while it has no effect on its reactivity towards H₂O. The findings of Rodriguez et al. [25] can also explain the reactivity profile obtained for char prepared in a CO₂-containing pyrolysis atmosphere which exhibits a higher reactivity in the first stages of the reaction (developed microporosity) and which decreases up to 40% of conversion due to burn-off. The increase in the reactivity from 40% to 50% of conversion is due to a developed char porosity and a higher catalytic activity

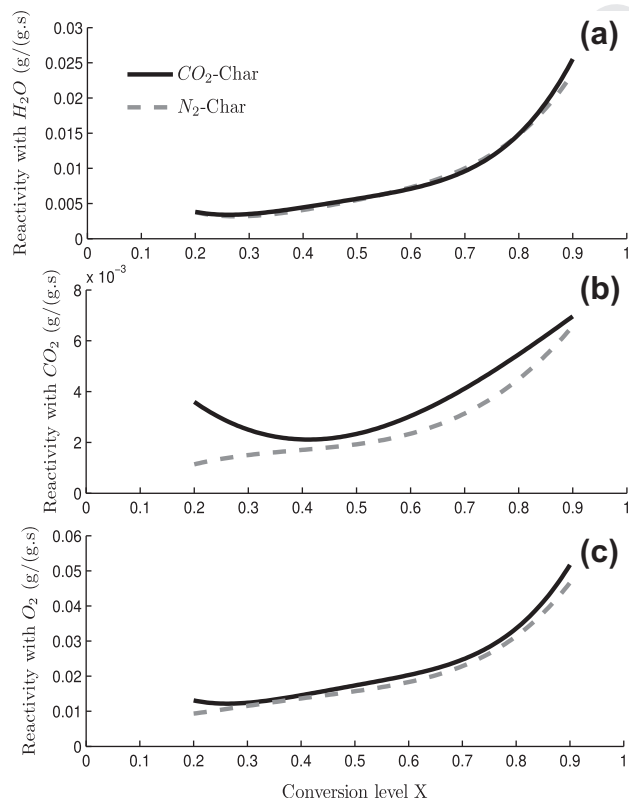


Fig. 8. Influence of the pyrolysis atmosphere on the char reactivity with (a) H₂O, (b) CO₂ and (c) O₂ at 850 °C (M-TG).

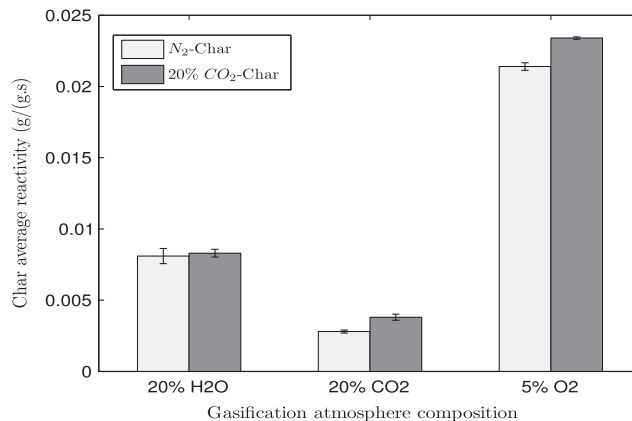


Fig. 9. Mean reactivities ($X = 0.2-0.9$) of N₂-char and CO₂-char towards H₂O, CO₂ and O₂ at 850 °C (M-TG).

Q1

C. Guizani et al./Fuel xxx (2013) xxx–xxx

9

of the minerals. Moreover, we found in our previous study on char gasification in mixed atmospheres of H₂O and CO₂ [14], that gasifying biomass chars with CO₂ up to 30% of conversion does not affect its reactivity towards H₂O, which corroborates the current findings.

In a fluidized bed, a major part of the char will be carried in the riser and combusted with air. With this in mind, we also performed combustion tests on the two chars with an oxygen concentration of 5% to assess the impact of the CO₂ during pyrolysis on the char reactivity with oxygen (Fig. 8.c). The average N₂-char and CO₂-char reactivities were respectively 0.0214 and 0.0234 with relative standard deviations below 5%. Average char reactivity results for the different gasification atmosphere are summarised in Fig. 9.

On the basis of these results we can conclude that the presence of CO₂ during pyrolysis mainly affects the char reactivity towards CO₂ and, to a lesser extent, with O₂, but does not affect the steam gasification of the char.

3.3.2.3. Temperature programmed oxidation. Temperature programmed oxidation experiments were performed on both chars and brought relevant insights. Fig. 10 shows the outflow of CO₂ as a function of temperature. The two chars exhibited two different oxidation profiles: both signal shapes and peak temperatures are different. The peak temperatures are respectively 580 and 600 °C for the N₂-char and for the CO₂-char. For the CO₂-char TPO curve, a single peak is observed. On the contrary, the N₂-char TPO curve shows a more complex shape during signal increase and a last peak at 635 °C. We believe that the CO₂-char contains a single type of carbon material while the N₂-char may contain more.

The TPO profiles were modelled using one or several parallel reactions converting char into CO₂ and CO following:

$$\frac{dm_{char}}{dt} = -k_{(T)} \cdot m_{char} \quad (13)$$

The rate constants $k_{(T)}$ follow an Arrhenius law that gives:

$$k_{(T)} = A \cdot \exp\left(-\frac{E}{R \cdot T}\right) \quad (14)$$

A and E are the frequency factor [s⁻¹] and the activation energy [J/mol].

Fig. 11 a and b shows temperature programmed oxidation experimental profiles and models for the N₂-char and the CO₂-char. The CO₂-char oxidation is well described by a single reaction: this tends to show that it contains a single type of carbon. It was not possible to model the N₂-char oxidation with a single reaction. However, the oxidation reaction is well described – as reported in Table 4 – when assuming the presence of three types of carbons. The model reads:

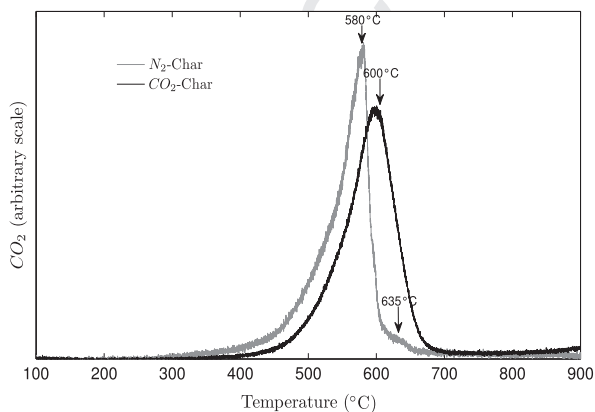


Fig. 10. TPO profiles of N₂-char and CO₂-char (HTR).

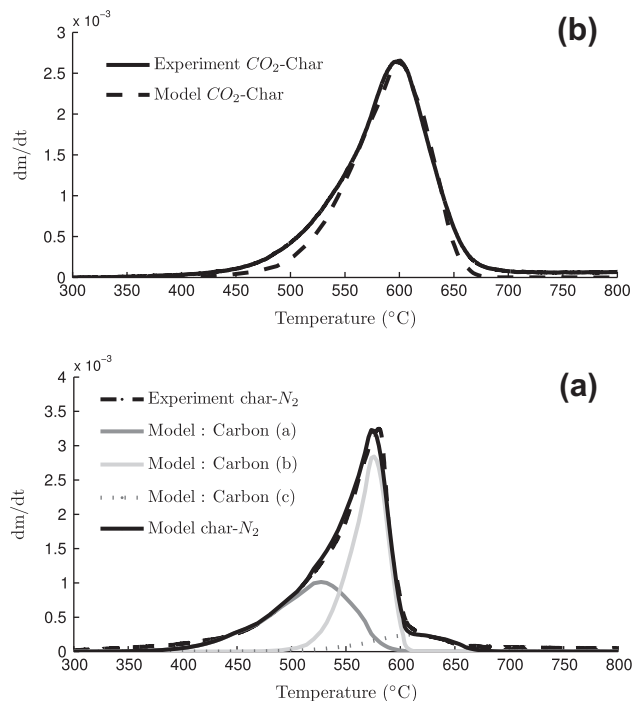


Fig. 11. TPO profiles modelling of N₂-char and CO₂-char.

Table 4
Temperature programmed oxidation kinetic parameters.

	CO ₂ -char	N ₂ -char		
		Carbon (a)	Carbon (b)	Carbon (c)
mass (g)	1	0.4	0.51	0.09
A_i (s ⁻¹)	12.10 ⁷	5.10 ⁶	6.10 ¹⁹	3.10 ⁸
E_i (kJ/mol)	170	135	350	190

$$\frac{dm_{char-N_2}}{dt} = -k_{1(T)} \cdot m_{carbon-a} - k_{2(T)} \cdot m_{carbon-b} - k_{3(T)} \cdot m_{carbon-c} \quad (15)$$

where $m_{carbon-a}$, $m_{carbon-b}$ and $m_{carbon-c}$ are the amount of carbon materials.

The frequency factors A_i and the activation energies E_i were identified by fitting the model to the experimental results.

The identified carbon masses, frequency factors and activation energies for the two chars are given in Table 4. The N₂-char appears to be composed of approximately 40% of a carbon with a small activation energy of 135 [kJ/mol], 51% of a high activation energy carbon 350 [kJ/mol] and 9% of a third carbon having an activation energy lying between these to values 190 [kJ/mol]. The activation energies of the first and the third carbons lie in the activation energy range for the lignocellulosic char-O₂ reaction (76–229 [kJ/mol]) given in Di Blasi's review [2]. However the second carbon has a higher activation energy in addition to a quite high pre-exponential factor. With an activation energy of 170 [kJ/mol], the oxidation reaction of the CO₂-char is typical of lignocellulosic biomass chars.

With regard to these results, the CO₂ may inhibit the last peak char formation by reacting with the tars, and therefore hinder their deposition and secondary char formation. The tars may have also been deposited on the char surface and removed afterwards by gasification. The last peak corresponds to the most stable form of carbon amongst the three identified forms. Logically, it should be the most difficult form to remove by gasification with CO₂, unless it is deposited on the char surface and is thus exposed first to this gasifying agent. A fact worth noting is that the mass of this third

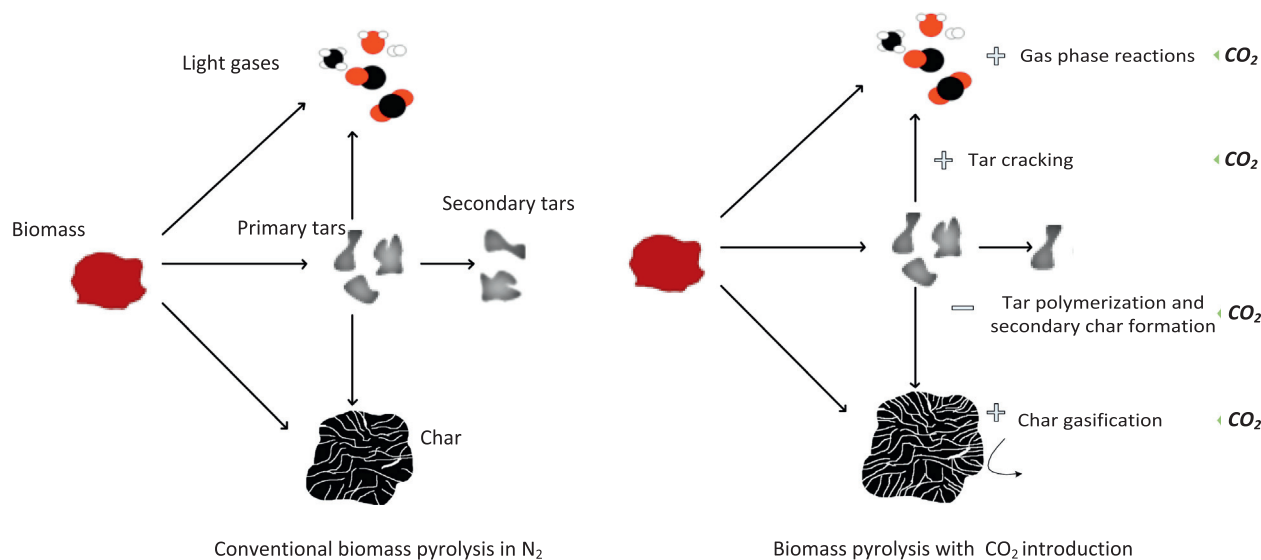


Fig. 12. The potential mechanisms in biomass pyrolysis with CO₂ introduction in the pyrolysis bath gas.

form of carbon corresponds to 10% of the total char mass, giving the TPO results. A link may be established with char mass decay observed in the MTG and HTR experiments when introducing CO₂. This char mass decay was in the range of 10–13%. Concerning the two other forms of carbon, introducing CO₂ may have changed the mechanisms of char formation and led consequently to another type of char. It is clear that we cannot go beyond assumptions at this level. These interpretations constitute a starting point towards highlighting the effect of CO₂ on the char properties and formation mechanisms.

4. Synthesis

Introducing CO₂ in the pyrolysis process atmosphere causes additional mass decay of the residual solid by 10 to 13% compared to pyrolysis in pure N₂. This mass decay can be explained either by char gasification by CO₂, which overlapped with the biomass pyrolysis, or by the fact that CO₂ hinders polymerisation reaction and secondary char formation by reacting and breaking some tar compounds that may lead to its formation. The mass decay is associated with an increase in the final permanent gas yield. With regard to the char ultimate analysis, the CO₂ seems to have an affinity to react with hydrogenated and oxygenated groups, leading to a more carbon-rich char, as amounts of these elements decreased in the CO₂-char. Finally, we observed an almost sixfold increase in char specific area. These observations are probably well correlated. In Fig. 12, we propose a representation of the potential effect of CO₂ when introduced in the pyrolysis bath gas and its interaction with the pyrolysis products.

The following scenario could be assumed as an interpretation for the different experimental observations and literature findings:

During the pyrolysis process, the CO₂ reacts with tars and enhances their cracking into light gases. This results in an increase in the gas yield and a reduction in tar polymerisation, which is behind the secondary char formation. A more homogeneous carbon-rich char with an enhanced microporosity is obtained. The TPO experiments tend to confirm this assumption: the TPO profile in the case of the CO₂-char is best described by a single reaction pathway, while the N₂-char exhibits several peaks, one of which may be imputable to the secondary char (carbon deposit). This carbon deposit is likely to contain a significant amount of hydrogenated and oxygenated groups and is probably deposited at the entry of the char pores, resulting in a lower surface area of the char.

5. Conclusion

CO₂ clearly has an influence during the biomass fast pyrolysis process. Its effects can be seen at two main levels: the pyrolysis gas yield and composition, and the char yield and properties. Introducing CO₂ induces an increase in CO concentration of the pyrolysis gas as a result of homogeneous and heterogeneous reactions of CO₂ with gases, tars and char. The char produced is also different and has high specific surface compared to a char obtained in N₂ atmosphere. TPO experiments show more than a single char oxidation peak in the N₂ char and sustain the assumption of tar polymerisation and secondary char formation. The CO₂ would appear to impede the secondary char formation and hinder tar polymerisation reactions.

Acknowledgements

The authors acknowledge the national research agency ANR-France for its financial support in the RECO2 project. They also wish to express their appreciation to Bernard Auduc for his technical support. Finally, the authors would also like to thank Laurent Bedel, Sylvie Valin and Claire Courson for their assistance and insightful conversations.

Appendix A. Determination of the heat transfer coefficients in the M-TG and HTR reactors

We drilled a steel ball of 1 cm diameter and inserted a thermocouple (K-type) at its centre. The ball was then placed in the basket that normally bears the biomass sample and introduced in the reactor the same way as in pyrolysis experiments. The temperature gradient inside the steel ball is negligible with a Biot number inferior to 0.1 and is therefore considered to be isothermal. An overall energy balance on the steel ball gives:

$$\rho_b \times V_b \times Cp_b \times \frac{dT}{dt} = h_{global} \times S_b \times (T_b(t) - T_\infty) \quad (A.1)$$

The ball's temperature evolution with time is given by:

$$\frac{T_b(t) - T_\infty}{T_b(0) - T_\infty} = \exp\left(-\frac{h_{global} \times S_b}{\rho_b \times V_b \times Cp_b} \times t\right) \quad (A.2)$$

The thermal time constant τ or characteristic time, representing the required time for the ball to reach 63% of the environment temperature is defined by:

Q1

$$\tau = \frac{\rho_b \times V_b \times Cp_b}{h_{global} \times S_b} \quad (A.3)$$

τ is determined experimentally. Knowing the physical characteristics of the steel ball, we can calculate the global heat transfer coefficient h_{global} according to the previous formula. The validity of this method can be verified by calculating the Biot number which represents the ratio of the internal thermal resistance to the boundary layer thermal resistance and must be inferior to 0.1:

$$Bi = \frac{h_{global} \times d_b}{\lambda_b} \quad (A.4)$$

The Biot numbers are respectively 0.06 and 0.09.

The heat transfer inside the two reactor occurs by convection and radiation. The global heat transfer coefficient is the sum of a convective and a radiative heat transfer coefficient:

$$h_{global} = h_{conv} + h_{rad} \quad (A.5)$$

To determine the contribution of each mode to the global heat transfer, we calculated the convective heat coefficient and determined the radiative coefficient by difference. The convective heat transfer coefficient is given by:

$$h_{conv} = \frac{Nu \times \lambda_{N_2}}{d_b} \quad (A.6)$$

where λ_{N_2} [W/m K] and d_b [m] are respectively the thermal conductivity of nitrogen at the reactor temperature and the steel ball diameter. The Nusselt number can be determined by the Whitaker correlation for flow over a spherical body [15]:

$$Nu = 2 + 0.4 \times (Re^{0.5} + 0.06 \times Re^{2/3}) \times Pr^{0.4} \quad (A.7)$$

where Re and Pr are respectively the Reynolds and the Prandtl numbers given by:

$$Re = \frac{\rho_{N_2} \times u_{\infty} \times d_b}{\mu_{N_2}} \quad (A.8)$$

$$Pr = \frac{\mu_{N_2} \times Cp_{N_2}}{\lambda_{N_2}} \quad (A.9)$$

where u_{∞} [m/s] is the average gas velocity, μ_{N_2} [Pa s] the nitrogen dynamic viscosity and Cp_{N_2} [J/kg K] the nitrogen specific heat capacity.

Appendix B. Determination of the particle heating rate in the M-TG and HTR reactors

For a biomass particle introduced in the reactor hot zone, its surface heating rate at $t = 0$ can be calculated following the next relation [16]:

$$\beta_0 = \frac{\partial T}{\partial t} \Big|_{t=0} = (T_{\infty} - T_{w,0}) \times \frac{h_{global}}{L_0 \times \rho_w \times Cp_w} \quad (B.1)$$

where L_0 [m] is the characteristic size, $\rho_w = 710$ [kg/m³], $Cp_w = 1500$ [J/kg K] and $\lambda_w = 0.18$ [W/m K] are respectively the wood density, specific heat value and conductivity. These physical properties are estimated from the literature [3].

References

- [1] Basu Prabir. Biomass gasification and pyrolysis, practical design and theory. Elsevier; 2010.
- [2] Di Blasi Colomba. Combustion and gasification rates of lignocellulosic chars. *Progr Energy Combust Sci* 2009;35(2):121–40.
- [3] LI CHEN. Fast Pyrolysis of millimetric wood particles between 800 °C and 1000 °C. PhD thesis, Université Claude Bernard - Lyon 1, 2009.
- [4] Mermoud F, Salvador S, Van de Steene L, Golfier F. Influence of the pyrolysis heating rate on the steam gasification rate of large wood char particles. *Fuel* 2006;85:1473–82.
- [5] Zhang Huiyan, Xiao Rui, Wang Denghui, He Guangying, Shao Shanshan, Zhang Jubing, et al. Biomass fast pyrolysis in a fluidized bed reactor under N², CO², CO, CH⁴ and H² atmospheres. *Bioresour Technol* 2011;102(5):4258–64.
- [6] Kwon Eilhann E, Jeon Young Jae, Yi Haarkho. New candidate for biofuel feedstock beyond terrestrial biomass for thermo-chemical process (pyrolysis/gasification) enhanced by carbon dioxide (CO²). *Bioresour Technol* 2012;123:673–7.
- [7] Kwon Eilhann E, Yi Haarkho, Castaldi Marco J. Utilizing carbon dioxide as a reaction medium to mitigate production of polycyclic aromatic hydrocarbons from the thermal decomposition of styrene butadiene rubber. *Environ Sci Technol* 2012;46(19):10752–7.
- [8] Hanaoka Toshiaki, Sakanishi Kinya, Okumura Yukihiko. The effect of N²/CO²/O² content and pressure on characteristics and CO² gasification behavior of biomass-derived char. *Fuel Process Technol* 2012;104(0):287–94.
- [9] Jamil Kawser, Hayashi Jun-ichiro, Li Chun-Zhu. Pyrolysis of a Victorian brown coal and gasification of nascent char in CO² atmosphere in a wire-mesh reactor. *Fuel* 2004;83(7-8):833–43.
- [10] Gao Song-ping, Zhao Jian-tao, Wang Zhi-qing, Wang Jian-fei, Fang Yi-tian, Huang Jie-jie. Effect of CO² on pyrolysis behaviors of lignite. *J Fuel Chem Technol* 2013;41(3):257–64.
- [11] Borrego AG, Garavaglia L, Kalkreuth WD. Characteristics of high heating rate biomass chars prepared under N² and CO² atmospheres. *Int J Coal Geol* 2009;77:409–15.
- [12] Gil MV, Riaza J, Ivarez L, Pevida C, Pis JJ, Rubiera F. Oxy-fuel combustion kinetics and morphology of coal chars obtained in N² and CO² atmospheres in an entrained flow reactor. *Appl Energy* 2012;91(1):67–74.
- [13] Rathnam Renu Kumar, Elliott Liza K, Wall Terry F, Liu Yinghui, Moghtaderi Behdad. Differences in reactivity of pulverised coal in air (O²/N²) and oxy-fuel (O²/CO²) conditions. *Fuel Process Technol* 2009;90(6):797–802.
- [14] Guizani C, Escudero Sanz FJ, Salvador S. The gasification reactivity of high-heating-rate chars in single and mixed atmospheres of H²O and CO². *Fuel* 2013.
- [15] Fundamentals of heat and mass transfer. DON Fowley; 2011.
- [16] Lede Jacques. Biomass pyrolysis: comments on some sources of confusions in the definitions of temperatures and heating rates. *Energies* 2010.
- [17] Jeguirim Mejdi, Trouve Gwenaëlle. Pyrolysis characteristics and kinetics of arundo donax using thermogravimetric analysis. *Bioresour Technol* 2009;100(17):4026–31.
- [18] Guerrero M, Ruiz MP, Alzueta MU, Bilbao R, Millera A. Pyrolysis of eucalyptus at different heating rates: studies of char characterization and oxidative reactivity. *J Anal Appl Pyrol* 2005;74:307–14.
- [19] Ahmed I, Gupta AK. Characteristics of cardboard and paper gasification with CO². *Appl Energy* 2009;86(12):2626–34.
- [20] Gilbert P, Ryu C, Sharif V, Swithenbank J. Tar reduction in pyrolysis vapours from biomass over a hot char bed. *Bioresour Technol* 2009;100(23):6045–51.
- [21] Zhang Li xin, Matsuhara Toru, Kudo Shinji, Hayashi Jun ichiro, Norinaga Koyo. Rapid pyrolysis of brown coal in a drop-tube reactor with co-feeding of char as a promoter of in situ tar reforming. *Fuel* 2011(0).
- [22] Sutton D, M Parle S, H Ross JR. The CO² reforming of the hydrocarbons present in a model gas stream over selected catalysts. *Fuel Process Technol* 2002;75(1):45–53.
- [23] Klinghoffer Naomi B, Castaldi Marco J, Nzihou Ange. Catalyst properties and catalytic performance of char from biomass gasification. *Indus Eng Chem Res* 2012;51(40):13113–22.
- [24] Marsh Harry, Rodriguez-Reinoso Francisco. Activation processes (thermal or physical). Oxford: Elsevier Science Ltd.; 2006 [Chapter 5].
- [25] Rodriguez-Reinoso F, Molina-Sabio M, Gonzalez MT. The use of steam and CO² as activating agents in the preparation of activated carbons. *Carbon* 1995;33(1):15–23.
- [26] Mohamed Abdul Rahman, Mohammadi Maedeh, Darzi Ghasem Najafpour. Preparation of carbon molecular sieve from lignocellulosic biomass: a review. *Renew Sust Energy Rev* 2010;14(6):1591–9.